Original Article

Sensitivity Analysis of a 6 MeV Photon Beam Monte Carlo Model

Nahid Shami[1], Maryam Atarod[2], Parvaneh Shokrani[1], Nadia Najafizade[3]

[1]Department of Medical Physics, School of Medicine, Isfahan University of Medical Sciences, Isfahan, Iran, [2]School of Allied Medical Sciences, Shahrekord University of Medical Sciences, Shahrekord, Iran, [3]Department of Radiooncology, School of Medicine, Isfahan University of Medical Sciences, Isfahan, Iran

Abstract

Background: This study aimed to optimize efficiency in Monte Carlo (MC) simulation using sensitivity analysis of a beam model. **Methods:** The BEAMnrc-based model of 6 MV beam of a Siemens Primus linac was developed. For sensitivity analysis, the effect of the electron source, treatment head, and virtual phantom specifications on calculated percent depth dose (PDD) and lateral dose profiles was evaluated. **Results:** The optimum mean energy (E) and the full width at half maximum (FWHM) of the intensity distribution of the electron beam were calculated as 6.7 MeV and 3 mm, respectively. Increasing E from 6.1 to 6.7 MeV, increased the PDD in the fall-off region by 4.70% and decreased the lateral profile by 8.76%. Changing the FWHM had a significant effect on the buildup region of PDD and the horns and out-of-field regions of the lateral profile. Increasing the collimators opening by 0.5 mm, PDD increased by 2.13% and the central and penumbra regions of profiles decreased by 1.98% and 11.40% respectively. Collimator properties such as thickness and density were effective in changing the penumbra (11.32% for 0.25 cm increment) and the out-of-field (22.82% for 3 g/cm^3) regions of the lateral profiles. **Conclusion:** Analysis of a 6 MV model showed that PDD profiles were more sensitive to changes in energy than to FWHM of the electron source. The lateral profiles were sensitive to E, FWHM, and collimator opening. The density of the collimator affected only the out-of-field region of lateral profiles. The findings of this study may be used to make benchmarking of an MC beam model more efficient.

Keywords: *Benchmarking, gamma analysis, monte carlo, radiotherapy, siemens primus*

Submitted: 29-Aug-2021 **Revised:** 21-Sep-2022 **Accepted:** 23-Mar-2023 **Published:** 29-May-2023

Introduction

Analytical dose calculation algorithms suffer from a clinically significant disagreement with measurement when treatment planning involves inhomogeneous areas.[1] These errors can become a dominant source of inaccuracy in treatment planning, especially in precision dose delivery techniques. Considering the uncertainties of dosimetry and treatment plan delivery, the importance of accurate dose calculations is highlighted. Monte Carlo (MC) techniques are considered the most accurate means of predicting dose distribution in inhomogeneous areas.[2]

Development and commissioning an MC model of the linear accelerator (linac)'s treatment head is a laborious task because detailed information about head structures and also the specification of the initial electron beam is typically proprietary. Even if these data are provided by the manufacturer, they are subject to manufacturing tolerances, adjustments following installation, and potential inaccuracies in the provided data.[3] Because of these restrictions, the simulation details are often adjusted in order to obtain an acceptable agreement between calculated and measured dose distributions. Benchmarking of the MC calculations can be time-consuming since the effective parameters of linac structures and electron beam properties are tuned using the trial and error method. However, the benchmarking process can become more targeted using sensitivity analysis of the calculated absorbed dose distributions to different parameters of linac and electron beam properties.[1,4-9]

Sheikh-Bagheri and Rogers have presented the mean energy and radial spread of an incident electron beam as the two most important parameters for simulating photon beams. They identified the lateral dose profiles as a sensitive tool for determining the radial intensity distribution of the initial electron beam and target material density.[3]

How to cite this article: Shami N, Atarod M, Shokrani P, Najafizade N. Sensitivity analysis of a 6 MeV photon beam Monte Carlo model. J Med Sign Sens 2023;13:144-52.

Address for correspondence:
Dr. Maryam Atarod, Department of Allied Medical Sciences, School of Medicine, Shahrekord University of Medical Sciences, Isfahan, Iran. E-mail: maryamatarod@yahoo.com

Access this article online

Website: www.jmssjournal.net

DOI: 10.4103/jmss.jmss_152_21

Quick Response Code:

Almberg *et al*. reported the effect of source size and jaw geometry on the width of the penumbra region of lateral profiles.[2] The effect of secondary collimator opening and its composition on penumbra and dose calculation results was shown in another study of Sheikh Bagheri and Rogers.[10] Keall *et al*. found that the target density does not play an important role in the determination of initial electron beam fluence[5] while Tzedakis *et al*. reported that the mean energy of the electron beam considerably affects depth dose and lateral dose distributions.[7] They also showed that lateral dose profile curves were affected by the radial intensity of the initial electron beam only for a large radiation field size and there is no influence of energy spread variations on either depth and lateral profiles. However, their comparisons were restricted to the umbra region of lateral dose profiles and to depths past the maximum dose for depth dose curves. The commissioning procedure of developed photon beam models, according to the manufacturer's blueprint, is very time-consuming even though it mainly requires manual tuning of initial electron beam parameters. Limited accessibility of researcher to the confident blueprint of linac, make this process more troublesome. The unknown geometry and structural data of Linac's components should be obtained during the trial-and-error method.

To facilitate the process of linac modeling without a manufacturer blueprint, it is necessary to know the sensitivity of the linac model to the less studied and uninvestigated geometrical and structural characteristics of the linac modules such as collimators as well as the virtual phantom voxel size in a different direction. To build the model that can be used to calculate the surface and out-of-field dose, model verification in regions of calculated profiles that are unusual in similar studies, such as the build-up and peripheral regions, is required. Therefore, this study was conducted to overcome some of the limitations in linac modeling without blueprint data, as explained above, and improves the model for additional applications such as surface and peripheral dose estimation. We performed a sensitivity analysis of calculated dose profiles obtained from a constructed model of Siemens Primus 6 MV photon beam using geometry and material specifications of treatment head structures, as well as electron beam and virtual phantom characteristics. The broad objective behind benchmarking the model was to reduce the number of simulations required to commission the developed photon beam model. However, our study's specific objective and nobility was to evaluate the number of less considered parameters such as density, thickness, and opening of collimators and virtual phantom's voxel size. Furthermore, in this study, the whole of the calculated dose distributions are considered in model validation, while in most of the studies, only the penumbra and fall-off regions have evaluated. Therefore, the results of this study can be used to optimize the commissioning process by reducing the effective parameters and minimizing the processing time. Other researchers can use the model generated during this study.

Materials and Methods

Development of a Monte Carlo model of siemens primus 6 MV photon beam

The MC model of 6 MV photon beam of a Siemens Primus medical linac (Siemens Medical Systems, Concord, CA, USA) was developed using the BEAMnrc[11] user code of EGSnrc[12] code system. The treatment head configuration elements were simulated using the following component modules (CMs) of BEAMnrc: SLABS for target, FLATFILT for flattening filter, SLABS for ionizing chamber, SLABS for mirror, JAWS for secondary collimators (Y and X), and VARMLC for multi-leaf collimators (MLC) [Figure 1]. Because of the negligible effect of the monitor chamber and mirror in photon beam interactions, the medium of these CMs was considered air in the simulations.[2,13]

The incident electron beam was considered to be mono-energetic and mono-directional, with an elliptical cross-section and a Gaussian radial intensity distribution (ISOURC = 19).[14]

Because of the lack of the manufacturer provided detailed information about the geometry and material composition of linac's components and electron source specifications, developing of the model was performed in a trial-and-error

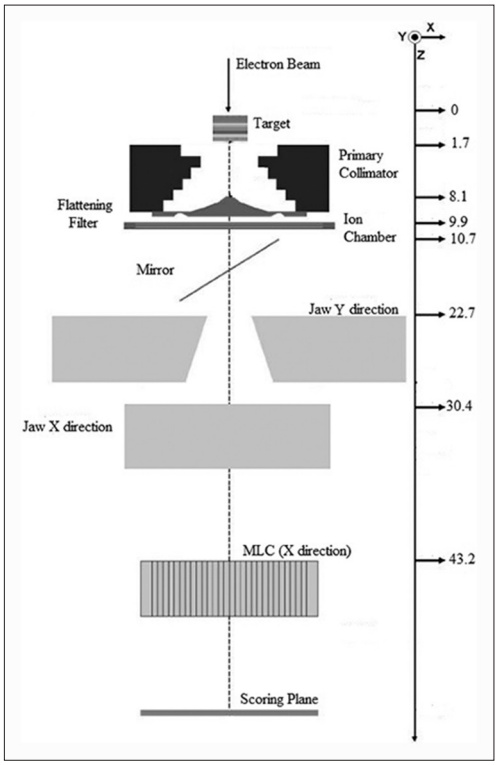

Figure 1: The preview of the Siemens Primus linac's head model, including distance of each component from the upper surface of the target as origin (This figure is not based on actual scale)

process. This process started with the available general data about Siemens linac components; nominal mean energy of E = 6 MeV and full width at half maximum (FWHM) of FWHM = 2 mm for intensity distribution of the electron beam. The geometry data of accessible components of linac such as jaws and MLCs were obtained through on-site physical measurements. In order to validate the source model, fine-tuning of electron beam parameters and treatment head components was done by matching the MC-calculated dose distributions of different field sizes with the measured ones. The field sizes were defined at the isocenter, located at z = 100 cm from the origin (upper surface of the target) in the BEAM user code.

Simulation parameters are chosen in Table 1. From variance reduction techniques, directional bremsstrahlung splitting, photon transport cutoff energy, electron transport cutoff energy, and electron range rejection were used to speed up the simulations.

Simulations were performed using two field sizes, 10 × 10 and 30 cm × 30 cm, and 4 × 10^7 histories for each field. A scoring plane was defined at Z = 71.2 cm below the MLC plane, in order to score the phase space data, i.e., the position, direction, energy, and type of the particles crossing this plane.

Dose calculations

Dose calculations were performed using the DOSXYZnrc user codes of EGSnrc codes system.[15] The scored phase space data in BEAMnrc were used as the source to calculate dose distributions in a water phantom. The 50 cm × 50 cm × 30 cm water phantom, designed using the DOSXYZnrc user code, was large enough in order to provide the conditions of full scatter for dose calculations along the beam axis [Figure 2]. Depending on the gradient of dose variations along the dose calculation axis, appropriate voxel sizes were used. For the build-up region of percent depth doses (PDDs), 0.2 cm × 1.0 cm × 0.1 cm and for other regions as well as for the lateral profile calculations 0.2 cm × 1.0 cm × 0.2 cm voxel sizes were used. PDDs and lateral dose profiles at depth of 10 cm were calculated for 10 cm × 10 cm and 30 cm × 30 cm fields and were normalized to the dose values at the d_{max} along the central axis. The cutoff energy in DOSXYZnrc was selected similar to BEAMnrc. The results of dose calculation in 3 ddose files were imported to stat dose, one of the EGSnrc subroutines, in order to plot the calculated dose distributions and to compare with the measured ones.

Table 1: Simulation parameters of BEAMnrc input file

Values	Parameters
ECUT	0.7 MeV
PCUT	0.01 MeV
Incident particles	4×10^7
Electron range rejection	0.8 MeV
Bremsstrahlung splitting	500 directional

ECUT – Electron transport cutoff; PCUT – Photon transport cutoff

Dose measurement

Dose measurements were performed using an automatic water phantom (Scanditronix, Wellhofer, Germany) and two 0.12 cm^3 ionization chambers (PTW-Freiburg, Germany), one as the reference and the other as the dose chamber. Measurements were done at a source-to-surface distance of 100 cm. The obtained data were corrected for the displacement of the effective measurement point of the chamber toward the phantom surface. The set of PDD curves and lateral beam profiles were measured with 1 mm resolution for the 10 × 10 and 30 cm × 30 cm field sizes.

Validation of the beam model

Beam model validation was done by comparing the calculated and measured depth and lateral profiles.[16] The tolerance limits recommended by IAEA in TRS430[17] and IAEA-TECDOC-1583[18,19] were used to validate the linac model as follows: 3% dose difference (DD) and 3 mm distance to the agreement.[20] The optimum combination of electron source specifications, i.e., E and FWHM, were determined by obtaining the best match between the calculated and measured depth and lateral dose profiles. The local DD method (gamma index) was used to enhance the sensitivity of the depth dose profile comparison.[3] The percentage difference between each point of calculated and measured distributions was calculated as follows:

$$\text{Relative dose difference (\%)} = \frac{(D_{Calculated} - D_{Measured}) \times 100}{D_{Measured}} \quad 1$$

Parameters influencing the beam models

In order to investigate the effect of incident electron beam and linac head components on depth and lateral dose distribution, dose calculations were performed with different sets of considered parameters. All lateral dose

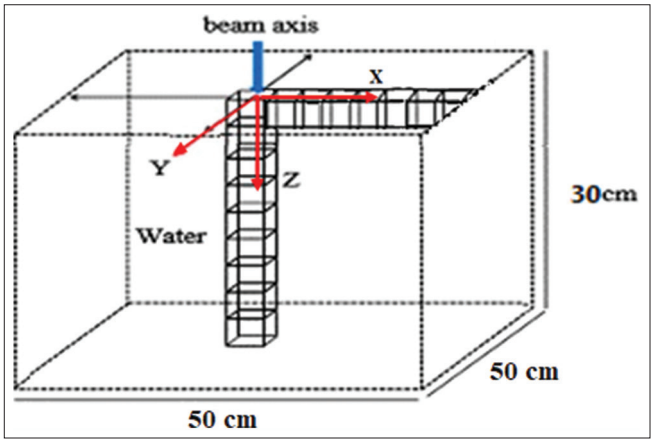

Figure 2: A simulated water phantom by DOSXYZnrc user code. The number and size of the voxels in the X, Y, and Z coordinates for PDD profile were 250 (0.2 cm), 50 (1 cm), and 158 (0.1 and 0.2 cm), respectively. PDD: Percent depth dose

profiles were obtained along the x-axis at 10 cm depth. To evaluate the sensitivity of calculated dose profiles to each parameter, only one parameter was changed and the rest of the parameters were kept constant. The initial electron beam parameters were set to E = 6.7 MeV and FWHM = 3 mm. The incident electron energy was changed from 6.1 to 6.7 MeV and FWHM varied from 0.1 to 4 mm with 1 mm step size.

The density of tungsten for the secondary collimators and MLCs was changed from 17 to 20, using 1steps. EGSnrc user code was used to generate the ICRU700 library (the pegs data) for different tungsten alloys.[21]

In order to obtain the best fit between measured and calculated profiles, the collimator opening was by 0.5 mm steps.

The effect of collimator thickness on calculated lateral dose profiles was evaluated by changing this parameter using 0.25 cm step sizes.

Lateral dose profile calculations were done along the x-axis with different voxel sizes in the homogenous water phantom. The dimensions of voxels in y and z directions for all calculations were 1 and 0.2 cm, respectively.

Results

Validation of the beam model

The calculated beam model was validated by comparing the calculated and measured PDD's. The optimal values for electron energy and FWHM for each investigated field size were determined using the energy range of 5.8–6.7 MeV with 0.1 MeV steps and considering a 95% passing rate. The calculated data points were approved if $\gamma \leq 1.0$ and failed if $\gamma > 1.0$. The γ index values obtained by comparing the calculated and measured PDD and lateral profiles of 10 cm × 10 cm and lateral profile of 30 cm × 30 cm filed size were 99.20%, 100%, and 96.70%, respectively. The model validation, illustrated in Figure 3, resulted in the optimum values of 6.7 ± 0.1 MeV and 3.0 ± 0.1 mm, for electron energy and FWHM respectively.

Different E (5.8–6.7 MeV with the 0.1 MeV step) of monoenergetic incident electron beam are illustrated in Figure 4.

Table 2 summarizes the resulting maximum and mean relative DDs between calculated and measured lateral dose profiles in central and penumbra regions of a 30 cm × 30 cm field, for energies in the considered limits of E. With respect to these data an optimum E of 6.7 MeV was obtained.

Tuning of full width at half maximum

Figure 5a shows the comparison of calculated lateral profiles with varying FWHM values in the range of 1–4 mm with 1 mm increment and 6.7 MeV E for 30 cm × 30 cm field in 10 cm depth with measured data. The relative deviation from the measured dose profile is shown in Figure 3.

The results of this study were in agreement with those of previous studies reporting that variations of the electron mean energy showed a larger impact on depth dose than lateral profiles, whereas lateral profiles were more sensitive to variations of the radial FWHM.

Thickness, opening, and density of secondary collimators

Density

Figure 6 shows the impact of secondary collimators density variation, by 1 steps, on calculated lateral dose profile of 30 cm × 30 cm field. Depth dose data is shown in Table 3.

Collimator's opening

The effect of secondary collimator's opening on dose profiles is shown in Figure 7. The best fit for calculated lateral dose profiles of 30 cm × 30 cm field was obtained with 3.50 and 4.72 cm collimator's opening for X and Y jaws, respectively.

Collimator thickness

The sensitivity of calculated dose profiles to collimator thickness is shown in Figure 8 and Depth dose data is shown in Table 4.

Virtual phantom voxel size

The effect of selecting different voxel sizes along the x-axis (cm) of the virtual phantom on dose profiles is shown in Table 5.

Uncertainty in the commissioning process

The uncertainties in the measurement using chamber and water phantom were caused by errors in the definition of phantom origin and water level adjustment for a vertical beam and ranged from 0.12%–0.25%.[22]

Uncertainties in dose calculation were as follows: Statistical uncertainties (0.53%), uncertainty related to the number of uncorrelated events and uncertainties caused by using an approximate geometry and spectrum for the electron source and other component modules. The combined standard uncertainty of the MC calculation yields 0.78% as a conservative estimate.[23]

Discussion

In this study, we investigated the relationship between the calculated dose distribution and the initial electron beam parameters, secondary collimator specifications, and virtual phantom's voxel size, with the goal of making the MC model commissioning more efficient. We commissioned the BEAMnrc model of a Siemens Primus 6 MV photon beam. All gamma values were smaller than 1. The maximum mean relative difference of 11.53% from measured data

Table 2: The mean and maximum relative dose difference between lateral dose profiles calculated using different electron energy values at 10 cm depth of water phantom and measured data in central and penumbra regions of 30 cm×30 cm field

Electron energy (MeV)	Penumbra region		Central region		Gamma rate (%)
	Maximum RDD (%)	Mean RDD (%)	Maximum RDD (%)	Mean RDD (%)	
6.1	25.31	11.53	8.65	2.53	68.00
6.3	22.84	11.63	10.11	2.57	66.30
6.5	19.72	11.66	7.11	1.07	98.80
6.7	18.10	11.53	2.93	0.88	100.00

RDD – Relative dose difference

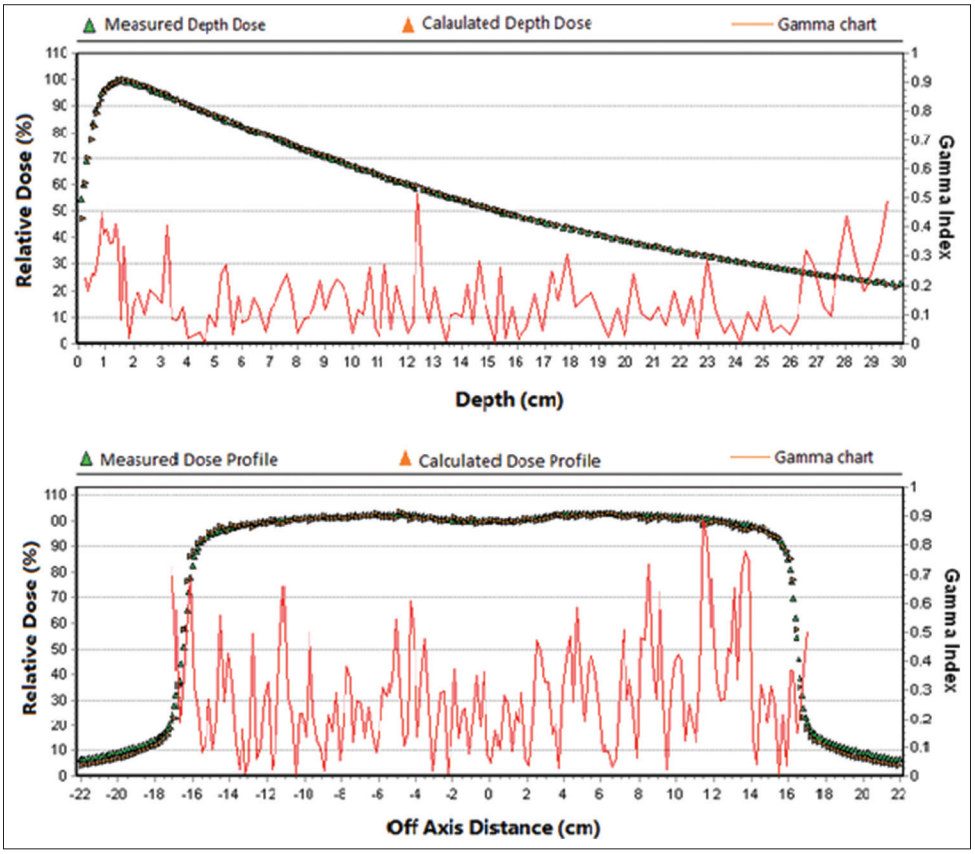

Figure 3: Comparison of measured and calculated dose distributions for 10 cm × 10 cm (above) and 30 cm × 30 cm (below) field sizes, calculated using 6.7 MeV and 0.3 cm for energy and FWHM, respectively. The gamma values for a 3mm/3% criterion are shown in solid lines. FWHM: Full width at half maximum

was seen in the penumbra region of the 30 cm × 30 cm cross-line profile calculated using the optimal electron beam parameters.

The maximum and average relative DDs between calculated and measured depth dose profiles, for E values in the stated range (6.1–6.7 MeV), were 13.22% and 4.34%, respectively. The minimum average relative DD can be seen for 6.4–6.7 MeV E values. The best agreement (average relative deviation of 0.84%) between the calculated and measured depth profiles was obtained using a 6.7 MeV mean energy for the electron beam. As the E increased from 6.1 MeV to 6.7 MeV, the relative dose in the fall-off region of calculated PDD increased on average by 4.70%. For the same energy range, the largest relative difference between measured and calculated dose profiles was 10.99% for the fall-off of PDD and 37.26% for the umbra region of lateral dose profiles. Therefore, the maximum relative difference between measured and calculated PDD was more sensitive to the variation of Park *et al*. reported an average increase of 4.36% in the calculated PDD curve by increasing the mean energy from 5.6 to 6.4 MeV. However, instead of using the measured PDD as the reference, their reference was the PDD calculated using the initial electron beam mean energy of 6 MeV.[24]

The agreement in the surface region of the depth dose profile was not as acceptable as in other regions. When measurements are done using a cylindrical chamber, correction for the effective point of measurement makes a

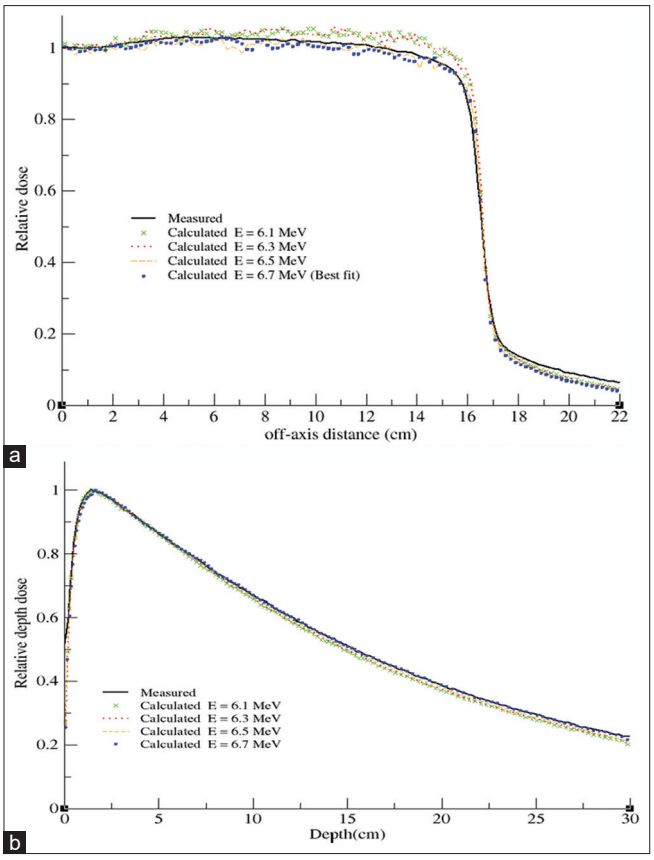

Figure 4: Comparing measured and calculated lateral dose profile (a) and PDD (b) for 30 cm × 30 cm field at 10 cm depth of the water phantom using varying E values (6.1–6.7 MV). PDD: Percent depth dose

critical difference in the build-up region, especially when normalization is done at locations deeper than the depth of the maximum dose.[25]

Increasing E by 0.2 MeV changed the relative dose in both central and penumbra regions of calculated lateral profiles of 30 cm × 30 cm field at depth = 10 cm of water phantom. The relative dose value in the horn regions decreased by 8.76% when the incident electron mean energy increased from 6.1 MeV to 6.7 MeV. By increasing E, the higher energy bremsstrahlung photons are scattered more forwardly and therefore the delivered dose to the horn region reduces. These findings show that compared to PDD curves, lateral dose profiles are more sensitive to electron energy. In a similar study, the maximum DD in the horn region was approximately 9.21% when energy increased by 0.4 MeV.[24] As Keall *et al*. study shows, by increasing electron beam energy, d_{max} is transferred to depth, and the horns of the lateral dose profile decrease.

The best fit for lateral dose profiles was obtained with 3 mm FWHM. By increasing the FWHM from 1 mm to 4 mm, the relative dose in the build-up region of the PDD profile decreased by an average of 0.20%. Variation of the FWHM parameter did not significantly change the relative dose in the fall-off region of the depth profile. We

Table 3: The (relative dose difference) between calculated percent depth dose profiles using 6 MV model designed with different density of secondary collimators and measured data in build-up and fall-off regions of 10 cm×10 cm field

Density of secondary collimators (g/cm^3)	Mean RDD (%)	
	Build-up region	Fall-off region
17	30.04	0.56
18	30.20	0.65
19	30.15	0.48
20	29.38	0.59

RDD – Relative dose difference

Table 4: The (relative dose difference) between calculated depth dose profile with different collimator thickness and measured data in build-up and fall-off regions of a 10 cm×10 cm field

Collimator thickness (cm)	Mean RDD (%)	
	Build-up region	Fall-off region
Optimum thickness +0.25	29.78	0.57
Optimum thickness +0.5	29.80	0.76
Optimum thickness +0.25	31.02	1.36
Optimum thickness +0.5	29.79	0.59

RDD – Relative dose difference

Table 5: The mean relative dose difference of calculated and measured cross-line lateral dose profiles of a 30 cm×30 cm field at depth of 10 cm using different voxel sizes along the x-axis of the virtual phantom

Region of the lateral profile	Size of voxels along the x-axis (cm)						
	0.1	0.2	0.3	0.5	0.7	1	1.5
Central	-	2.6	-	0.85	0.79	0.64	-
Penumbra	12.6	11.5	10.3	9.98	-	-	-
Umbra	-	24.1	-	23.8	-	21.7	19.8

These values were none selected as voxel dimension for dose calculation

observed a local minimum relative difference of 6.44% in average deviation for 3 mm FWHM in the lateral profile. The relative dose in horns, penumbra, and out-of-field regions of the calculated lateral profile decreased, remained constant, and increased, respectively, when a large FWHM was used [Figure 5a]. The PDD showed more sensitivity to E than to FWHM. As other studies found, the effect of change in FWHM on PDD is insignificant,[26,27] since by increasing FWHM of incident electron beam only the width of bremsstrahlung photons beam increases and its energy remains constant. Therefore, the PDD, which is mainly affected by photon energy, is not affected significantly by FWHM [Figure 5b]. Our results showed that the lateral profiles were sensitive to the mean energy, intensity distribution, and collimator's opening. By increasing both E and FWHM of incident electrons, the average dose values decreased throughout the lateral profiles. Similar to the findings of previous studies,[24] we

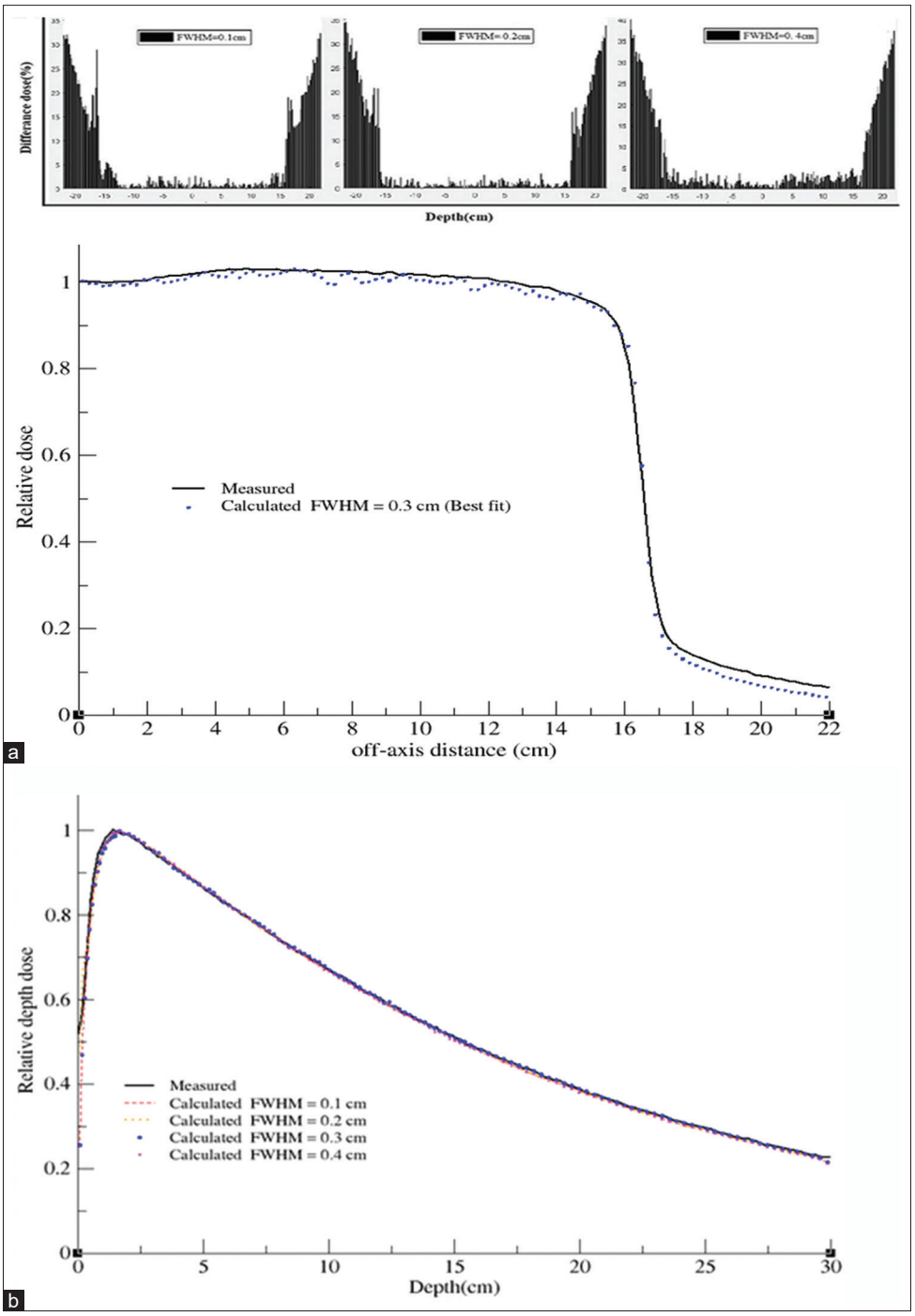

Figure 5: Comparison of (a) lateral dose profiles and (b) PDD calculated using E = 6.7 MeV and varying FWHM (1–4 mm) for a 30 cm × 30 cm field in 10 cm depth of the water phantom with measured data of a 6 MV photon beam. FWHM: Full width at half maximum, PDD: Percent depth dose

found that the shape of the lateral dose profile is influenced by the energy of the initial electron beam.

The relative dose in the central and penumbra regions of lateral profiles altered by 1.98% and 11.40% Ni, respectively, when the collimator opening increased by 0.5 mm.

The same variation in the collimator's opening changed the surface region of the PDD profile by 2.13%. As can be seen in Figure 8, The relative dose in the penumbra of the lateral profile altered by 11.32% and 11.18%, while the secondary collimator's thickness were increased and decreased 0.25 cm, respectively.

Our results showed that uncertainty related to the density of the secondary collimator affects the umbra region of lateral profiles. The impact of secondary collimator density variation from 17 to 20 , by 1 steps, on changing the mean

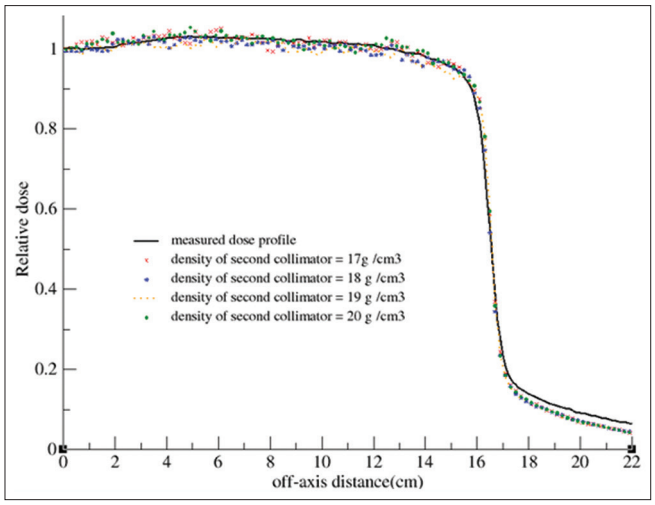

Figure 6: The effect of secondary collimator density on lateral dose profile of 30 cm × 30 cm field, (E = 6.7 MeV and FWHM = 0.3 cm). FWHM: Full width at half maximum

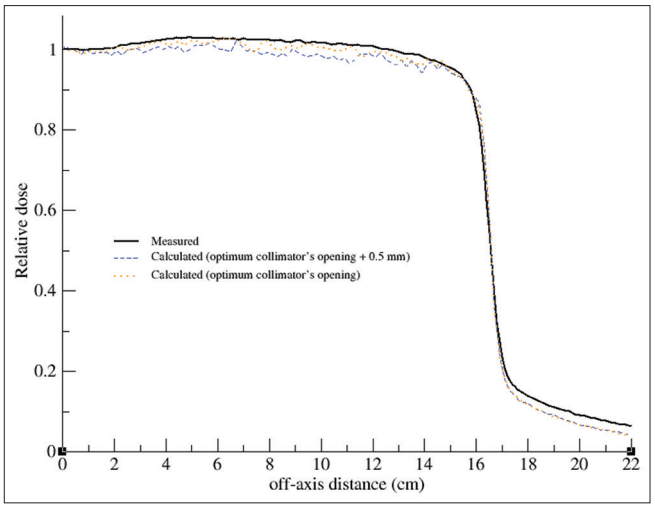

Figure 7: The effect of 0.5 mm increment in secondary collimators (X and Y jaws) opening related to optimum value on lateral dose profiles of 30 cm × 30 cm field (E = 6.7 MeV and FWHM = 0.3 cm). FWHM: Full width at half maximum

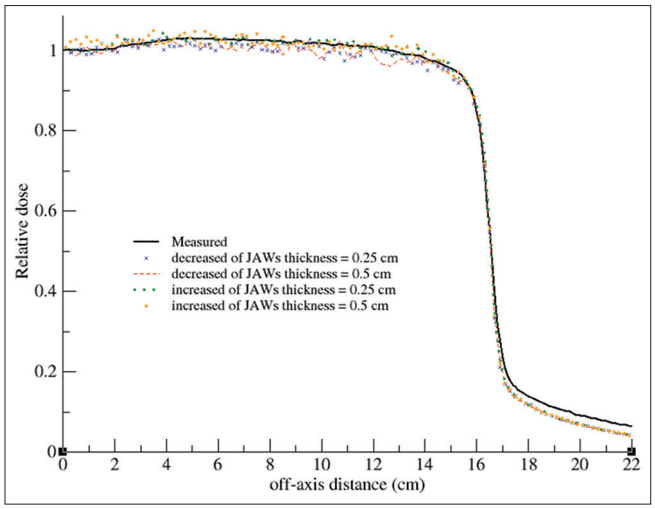

Figure 8: Sensitivity of calculated lateral dose profiles of 30 cm × 30 cm field to 0.25 cm increment changes in secondary collimator's thickness (E = 6.7 MeV and FWHM = 0.3). FWHM: Full width at half maximum

and maximum relative dose in out-of-field areas of lateral profiles were 22.82% and 37.80%, respectively. With respect to the considered gamma criteria for commissioning the photon model, these differences are not statistically significant. The dose in a penumbra region is deposited by transmitted radiation through the edges of the jaws and head shielding. Therefore, the dose in this region can be sensitive to the collimator's density. Sheikh-Bagheri and Rogers. found no difference in the obtained dose profiles using different jaw compositions, varied from pure tungsten to a tungsten alloy (consisted of 10.70% Cu, 32.20% Ni, 57.10% W).[3] However, they have not pointed to the relation of collimator's density and dose variations.

Our sensitivity analysis of calculated dose profiles to changes in virtual phantom voxel size showed that by increasing the virtual phantom voxel size, the mean relative DD decreased.

In this study, we investigated the sensitivity of an MC photon beam model to different parameters used in model commissioning. Our findings showed that incident electron energy is an effective parameter in both depth and lateral dose profiles. Thus, we recommend to adapt the overall depth and lateral profile shapes to the measured profiles by adjusting the E, and then fine-tuning can be done using the FWHM. Furthermore, collimator density and thickness had negligible effects on lateral and depth dose profiles.

Conclusion

The commissioned model of Siemens Primus 6MV photon beam developed in this study can be used for modeling of linacs of similar make, with some tuning if necessary. The parameters identified in this sensitivity analysis can make the developing of MC beam models of other linac brands more efficient.

Acknowledgment

This article is based on the master's research project with number 398415, which is the financial and credit source of the Isfahan University of Medical Sciences.

Financial support and sponsorship

None.

Conflicts of interest

There are no conflicts of interest.

References

1. Najafzadeh M, Hoseini-Ghafarokhi M, Bolagh RS, Haghparast M, Zarifi S, Nickfarjam A, *et al.* Benchmarking of monte carlo model of siemens oncor® linear accelerator for 18MV photon beam: Determination of initial electron beam parameters. J Xray Sci Technol 2019;27:1047-70.
2. Almberg SS, Frengen J, Lindmo T. Monte Carlo study of in-field

and out-of-field dose distributions from a linear accelerator operating with and without a flattening-filter. Med Phys 2012;39:5194-203.
3. Sheikh-Bagheri D, Rogers DW. Sensitivity of megavoltage photon beam Monte Carlo simulations to electron beam and other parameters. Med Phys 2002;29:379-90.
4. Tuğrul T, Eroğul O. Determination of initial electron parameters by means of Monte Carlo simulations for the siemens artiste linac 6 mv photon beam. rep pract oncol Radiother 2019;24:331-7.
5. Keall PJ, Siebers JV, Libby B, Mohan R. Determining the incident electron fluence for Monte Carlo-based photon treatment planning using a standard measured data set. Med Phys 2003;30:574-82.
6. Chang KP, Wang ZW, Shiau AC. Determining optimization of the initial parameters in Monte Carlo simulation for linear accelerator radiotherapy. Radiat Phys Chem 2014;95:161-5.
7. Tzedakis A, Damilakis JE, Mazonakis M, Stratakis J, Varveris H, Gourtsoyiannis N. Influence of initial electron beam parameters on Monte Carlo calculated absorbed dose distributions for radiotherapy photon beams. Med Phys 2004;31:907-13.
8. Mishra S, Dixit PK, Selvam TP, Yavalkar SS, Deshpande DD. Monte Carlo investigation of photon beam characteristics and its variation with incident electron beam parameters for indigenous medical linear accelerator. J Med Phys 2018;43:1-8.
9. Gündem E, Dirican B. Analysis of characteristics and validation of 6 MV photon beam produced by Elekta Synergy linear accelerator using EGSnrc Monte Carlo code. Radiat Phys Chem 2021;184:109491.
10. Sheikh-Bagheri D, Rogers DW. Monte Carlo calculation of nine megavoltage photon beam spectra using the BEAM code. Med Phys 2002;29:391-402.
11. Rogers DW, Walters B, Kawrakow I. BEAMnrc Users Manual NRCC Report PIRS-0509 (A) revL. Ottawa: National Research Council Canada; 2013.
12. Kawrakow I. The EGSnrc Code System, Monte Carlo Simulation of Electron and Photon Transport. NRCC Report Pirs-701; 2001.
13. Mahmoudi G, Farhood B, Shokrani P, Amouheidari A, Atarod M. Evaluation of the photon dose calculation accuracy in radiation therapy of malignant pleural mesothelioma. J Cancer Res Ther 2018;14:1029-35.
14. Gholampourkashi S, Cygler JE, Belec J, Vujicic M, Heath E. Monte Carlo and analytic modeling of an Elekta Infinity linac with agility MLC: Investigating the significance of accurate model parameters for small radiation fields. J Appl Clin Med Phys 2019;20:55-67.
15. Kawrakow I, Walters BR. Efficient photon beam dose calculations using DOSXYZnrc with BEAMnrc. Med Phys 2006;33:3046-56.
16. Mohammed M, El Bardouni T, Chakir E, Saeed M, Mohamed L. Validation of BEAMnrc Monte Carlo model for a 12 MV photon beam. J King Saud Univ 2018;30:537-43.
17. INTERNATIONAL ATOMIC ENERGY AGENCY, Commissioning and Quality Assurance of Computerized Planning Systems for Radiation Treatment of Cancer, Technical Reports Series No. 430, IAEA, Vienna (2004).
18. Rodríguez Linares, Deijany & Alfonso, Rodolfo & Fiandor, Juan. (2017). Comissioning of Radiotherapy Treatment Planning Systems: Optimization of the Dosimetric Test of the IAEA TECDOC-1583 guidelines. 10.13140/RG.2.2.22466.02248.
19. International Energy Agency. Commissioning of Radiotherapy Treatment Planning Systems: Testing for Typical External Beam Treatment Techniques TecDoc I. 1583. Vienna: International Energy Agency; 2008.
20. Bencheikh M, Maghnouj A, Tajmouati J. Energetic properties' investigation of removing flattening filter at phantom surface: Monte Carlo study using BEAMnrc code, DOSXYZnrc code and BEAMDP code. Phys Part Nucl Lett 2017;14:953-62.
21. Rogers DW, Walters B, Kawrakow I. BEAMnrc users manual. Nrc Rep Pirs 2009;509:12.
22. Kinoshita N, Kohno R, Oguchi H. Technical note: Influence of entrance window deformation on reference dosimetry measurement in various beam modalities. Med Phys 2019;46:1037-43.
23. Renner F, Wulff J, Kapsch RP, Zink K. Uncertainties in Monte Carlo-based absorbed dose calculations for an experimental benchmark. Phys Med Biol 2015;60:7637-53.
24. Park H, Choi HJ, Kim JI, Min CH. Analysis of dose distribution according to the initial electron beam of the linear accelerator: a Monte Carlo study. Journal of Radiation Protection and Research. 2018;43:10-9.
25. Sheikh-Bagheri D, Rogers DW, Ross CK, Seuntjens JP. Comparison of measured and Monte Carlo calculated dose distributions from the NRC linac. Med Phys 2000;27:2256-66.
26. López-Sánchez M, Pérez-Fernández M, Fandiño JM, Teijeiro A, Luna-Vega V, Gómez-Fernández N, *et al.* An EGS Monte Carlo model for varian trueBeam treatment units: Commissioning and experimental validation of source parameters. Phys Med 2019;64:81-8.
27. Soh RC, Tan LK, Goh MS, Yani S, Haryanto F, Siang W. A gamma analysis approach to determine optimal parameters for monte carlo simulation of 6MV varian clinac iX photon beam. J Health Sci 2017;5:36-43.